Journal of Neural Engineering

PAPER • OPEN ACCESS

Development and validation of a 3D-printed neuronavigation headset for therapeutic brain stimulation

To cite this article: Farrokh Mansouri *et al* 2018 *J. Neural Eng.* **15** 046034

View the article online for updates and enhancements.

Related content

- Electric field strength and focality in electroconvulsive therapy and magnetic seizure therapy: a finite element simulation study
- Combined rTMS and virtual reality brain–computer interface training for motor recovery after stroke
- Automated detection and labeling of high-density EEG electrodes from structural MR images

Recent citations

- Review of semi-dry electrodes for EEG recording
Guang-Li Li *et al*

PITT | SWANSON ENGINEERING
BIOENGINEERING

The Department of Bioengineering at the University of Pittsburgh Swanson School of Engineering invites applications from accomplished individuals with a PhD or equivalent degree in bioengineering, biomedical engineering, or closely related disciplines for an open-rank, tenured/tenure-stream faculty position. We wish to recruit an individual with strong research accomplishments in Translational Bioengineering (i.e., leveraging basic science and engineering knowledge to develop innovative, translatable solutions impacting clinical practice and healthcare), with preference given to research focus on neuro-technologies, imaging, cardiovascular devices, and biomimetic and biorobotic design. It is expected that this individual will complement our current strengths in biomechanics, bioimaging, molecular, cellular, and systems engineering, medical product engineering, neural engineering, and tissue engineering and regenerative medicine. In addition, candidates must be committed to contributing to high quality education of a diverse student body at both the undergraduate and graduate levels.

CLICK HERE FOR FURTHER DETAILS

To ensure full consideration, applications must be received by June 30, 2019. However, applications will be reviewed as they are received. Early submission is highly encouraged.

This content was downloaded from IP address 184.175.34.200 on 28/10/2020 at 14:35

OPEN ACCESS
IOP Publishing
Journal of Neural Engineering
J. Neural Eng. **15** (2018) 046034 (9pp)
https://doi.org/10.1088/1741-2552/aacb96

Development and validation of a 3D-printed neuronavigation headset for therapeutic brain stimulation

Farrokh Mansouri[1], Arsalan Mir-Moghtadaei[3], Vanathy Niranjan[5], Jian Shu Wu[2], Daniyar Akhmedjanov[2], Mishael Nuh[2], Terri Cairo[5,7], Peter Giacobbe[4,5,8], José Zariffa[1,6] and Jonathan Downar[3,4,5,7,9]

[1] Institute of Biomaterial and Biomedical Engineering, University of Toronto, Toronto, Canada
[2] Division of Engineering Science, University of Toronto, Toronto, Canada
[3] Institute of Medical Science, University of Toronto, Toronto, Canada
[4] Department of Psychiatry, University of Toronto, Toronto, Canada
[5] Centre for Mental Health, University Health Network, Toronto, Canada
[6] Toronto Rehabilitation Institute, University Health Network, Toronto, Canada
[7] Krembil Research Institute, University Health Network, Toronto, Canada
[8] Harquil Centre for Neuromodulation, Sunnybrook Health Science Centre, Toronto, Canada

E-mail: jonathan.downar@uhn.ca

Received 23 April 2018, revised 4 June 2018
Accepted for publication 11 June 2018
Published 27 June 2018

Abstract

Background. Accurate neuronavigation is essential for optimal outcomes in therapeutic brain stimulation. MRI-guided neuronavigation, the current gold standard, requires access to MRI and frameless stereotaxic equipment, which is not available in all settings. Scalp-based heuristics depend on operator skill, with variable reproducibility across operators and sessions. An intermediate solution would offer superior reproducibility and ease-of-use to scalp measurements, without requiring MRI and frameless stereotaxy. *Objective.* We present and assess a novel neuronavigation method using commercially-available, inexpensive 3D head scanning, computer-aided design, and 3D-printing tools to fabricate form-fitted headsets for individuals that hold a stimulator, such as an rTMS coil, in the desired position over the scalp. *Methods.* 20 individuals underwent scanning for fabrication of individualized headsets designed for rTMS of the left dorsolateral prefrontal cortex (DLPFC). An experienced operator then performed three trials per participant of three neuronavigation methods: MRI-guided, scalp-measurement (BeamF3 method), and headset placement, and marked the sites obtained. Accuracy (versus MRI-guidance) and reproducibility were measured for each trial of each method. *Results.* Within-subject accuracy (against a gold-standard centroid of three MRI-guided localizations) for MRI-guided, scalp-measurement, and headset methods was 3.7 ± 1.6 mm, 14.8 ± 7.1 mm, and 9.7 ± 5.2 mm respectively, with headsets significantly more accurate ($M = 5.1$, $p = 0.008$) than scalp-measurement methods. Within-subject reproducibility (against the centroid of 3 localizations in the same modality) was 3.7 ± 1.6 mm (MRI), 4.2 ± 1.4 (scalp-measurement), and 1.4 ± 0.7 mm (headset), with headsets achieving significantly better reproducibility than either other method ($p < 0.0001$). *Conclusions.*

[9] MRI-Guided rTMS Clinic Toronto Western Hospital 7M-415, 399 Bathurst Street, Toronto, ON M5T 2S8, Canada.

Original content from this work may be used under the terms of the Creative Commons Attribution 3.0 licence. Any further distribution of this work must maintain attribution to the author(s) and the title of the work, journal citation and DOI.

 © 2018 IOP Publishing Ltd Printed in the UK

3D-printed headsets may offer good accuracy, superior reproducibility and greater ease-of-use for stimulator placement over DLPFC, in settings where MRI-guidance is impractical.

Keywords: brain stimulation, rTMS, tDCS, neuronavigation, 3D printing, 3D scanning

(Some figures may appear in colour only in the online journal)

Introduction

Non-invasive brain stimulation techniques are emerging into clinical practice as alternatives to medications and psychotherapy in the treatment of psychiatric illnesses. A leading example is repetitive transcranial magnetic stimulation (rTMS). rTMS uses powerful (1–2 T), focused magnetic field pulses to induce durable changes in the activity of a target brain region. A course of 20–30 daily sessions, targeting brain regions that regulate cognition and emotion, may have antidepressant effects in cases where medications fail. rTMS is approved and funded in an increasing number of jurisdictions worldwide as a treatment for major depression, and is under study for a variety of other illnesses; it is also incorporated into formal clinical treatment guidelines in the USA, Canada and Europe among other regions [1–3]. Another example is transcranial direct current stimulation (tDCS), falling within the larger family of techniques for transcranial electrical stimulation (tES). tDCS relies on mild (1–2 mA) electrical currents to modulate the ongoing activity of brain regions near the surface, once again leading to both transient and more durable effects on the activity of the target brain region. Once again, a course of 15–30 daily sessions can have antidepressant effects comparable in some cases to those of conventional antidepressant medications. Although less widely available in clinical practice, tDCS has shown efficacy against depression in several large trials [4–6] and meta-analyses [7, 8]. Given the advantages of low cost, excellent tolerability, and the potential for at-home rather than in-clinic delivery, tES modalities may also enter more common clinical use over the next decade. A number of newly emerging brain stimulation techniques such as, TLS (transcranial laser/light stimulation) [9, 10] and TPU (transcranial pulsed ultrasound) [11] have the potential to become clinically available for neuropsychiatric disorders.

One key feature of non-invasive brain stimulation techniques is that they are anatomically specific in their effects. As such, their successful use requires both the judicious choice of a stimulation target in the brain, as well as a methodology for ensuring that the stimulation is delivered accurately to the desired location. For example, with rTMS in major depression, one of the most common targets is the dorsolateral prefrontal cortex (DLPFC), either left, right, or bilaterally [12–14]. With tDCS, likewise, stimulation is typically targeted upon the DLPFC in most large studies [7, 8]. Various theories exist regarding the role of the DLPFC target in depression, most proposing that it belongs to a network of brain regions that regulate cognition and/or emotional states [15, 16]. Failure to target the DLPFC accurately has been noted to result in a higher likelihood of non-response to treatment [15, 17].

To ensure that the intended area is stimulated, there are a variety of techniques currently in use for neuronavigation. On the low-cost end of the spectrum are heuristics based on scalp measurements. These include the classical '5 cm anterior to motor hotspot' heuristic often used for DLPFC-rTMS [18], and the more recent *BeamF3* method for localizing the F3 EEG sensor site in the international 10–20 system [19]; this site is a commonly used proxy for the DLPFC. We have previously reported [20] that a slightly modified BeamF3 heuristic shows good concordance with the current gold-standard approach, MRI-guided neuronavigation, with a discrepancy of 0.35–0.65 cm depending on which variation of the heuristic is applied. However, scalp-measurement-based methods are dependent upon the expertise of the operator, and may be variable in reproducibility both across operators and even across sessions for the same operator.

MRI-guidance offers the advantage of greater accuracy in neuronavigation to specific stereotaxically-or functionally-defined target brain regions, in individual patients. For this reason, MRI-neuronavigation may be the preferred technique for non-standard targets, or in research settings where field-modelling is contemplated. However, in clinical settings, it may not always be feasible to obtain an MRI for every patient undergoing rTMS, and frameless stereotaxic equipment is not universally employed. Moreover, given the ~2% prevalence of medication-resistant depression in the general population [21], a requirement for MRI in all patients could pose significant logistical and economic limitations on the real-world utility of rTMS as a practical tool to reduce the overall health burden of this disease. As such, there is a need for an intermediate method that improves upon the reproducibility and operator-dependence of scalp-based methods, while at the same time offering better cost, accessibility, and ease-of-use, for implementation in high-volume community clinical settings.

An opportunity to improve on current methods arises from two enabling technologies: 3D scanning and 3D printing. Formerly expensive and used primarily in industry, both of these technologies have improved dramatically in cost and quality as they have entered the broader consumer market over the last decade. Reasonable-quality off-the-shelf 3D scanners and printers may be obtained for as little as ~$1000–2000—lower than the cost of rTMS or tDCS equipment itself. 3D scanning technologies have potential applications to improve the precision of head measurement and site specification, while 3D printing could be applied to generate form-fitted crown headsets for holding the stimulation device in place, customized to the patient head shape. 3D printed, customized neuronavigation headsets can be positioned very quickly and reliably compared to frameless stereotaxy, are less dependent

Figure 1. A commercially available 3D scanner was used to 3D scan the subject's head. The subjects were rotated 360° in the field of view of the camera to complete a full 3D scan of their head and the captured mesh was edited and exported using freely available open-source MeshLab software.

on operator skill, and can be generated at low cost in large numbers with commercially available off-the-shelf equipment.

Here we introduce a novel methodology that combines 3D scanning, computer-aided design (CAD), and 3D printing to generate individualized neuronavigation crowns (headsets) for rTMS coil placement. We compare these headsets to gold-standard MRI-guided neuronavigation as well as to the *BeamF3* scalp heuristic on the metrics of accuracy, reproducibility, and procedure time. Finally, we discuss possible extensions of the methodology to other brain stimulation modalities such as tES.

Methods

Participants

20 healthy volunteers (13/7 male/female; mean age 27.4 ± SD 5.9 years, range 21–41) free of neurological or psychiatric illness participated in the study. All participants gave informed consent, and the study was approved by the Research Ethics Board of the University Health Network.

3D scanning

Participants underwent 3D head scanning using an inexpensive (<$1500 USD), commercially available Structural Sensor 3D scanner and associated software (Skanect Pro, ManCTL, France). Participants wore a close-fitting fabric scalp cap to hold the hair as close to the scalp as possible. Small protruding stickers were applied to mark the left and right tragus and inion during the 3D scanning session. For 3D shape capture, participants sat on a rotating stool and rotated through 360° over about 10 s in the field of view of the camera (figure 1). Next, the captured 3D mesh was processed in a mesh editing software (MeshLab [22]) to ensure the scalp surface model was smooth and free of flaws or inconsistencies.

Headset fabrication

The 3D head mesh file was loaded into MATLAB (MATLAB R2016a), and a trained technician experienced in rTMS identified the coordinate of inion, nasion and tragi points on the head model. Next, an in-house MATLAB script analyzed the 3D head model to trace the three cardinal scalp measurements (head circumference, inion-nasion and tragus–tragus distances). These were input into the *BeamF3* algorithm [19], applying the MRI-validated +0.35 cm extension of the radial measurement as per Mir-Moghtadaei *et al* [20], to define the left DLPFC stimulation target on the scalp surface near the EEG site F3 in the international 10–20 system (figure 2).

Following F3 localization, the MATLAB script then automatically constructed a personalized CAD model of a headset to place the stimulator coil over the defined site on the scalp mesh. The headset (shown in figure 3) consisted of a nosepiece formed to the participant's nasion, a horizontal half-ring formed to the participant's forehead with terminal hooks for fastening an elastic band to help hold the headset in place, a coil bracket centred on the left DLPFC scalp site and oriented at the standard 45° angle to midline, and a radial bracket formed to the right forehead and extending to the symmetrical right DLPFC scalp site to ensure a close fit of the crown. The left-sided and right-sided brackets had pinpoint holes at the exact left and right DLPFC sites to enable marking of the target spot on the scalp. This CAD model of the headset was used to 3D print the headset using an inexpensive (<$3000) commercially available 3D printer (FlashForge Creator Pro), with print time ~12 h.

Comparative assessment of navigation accuracy and reproducibility

After fabrication of the headset, participants returned for a second testing session comparing three methods (MRI-neuronavigated, scalp-landmark, and headset) to localize the stimulation target point. Each method was performed three times in each participant, to evaluate reproducibility and accuracy. During testing, participants wore a standard white fabric rTMS scalp cap, and the result from each trial was marked on the cap using invisible UV-fluorescent ink, so that subsequent trials would not be biased by the previous trials. The time required to complete each method was also recorded on all 3 trials for each participant.

MRI-Neuronavigation method

Each participant had previously undergone MRI on a 3 T GE Signa HDx scanner equipped with an 8-channel phased-array head coil. The anatomical scan was a T1-weighted fast spoiled gradient-echo (TE = 12 ms, TI = 300 ms, flip angle = 20°, 116 sagittal slices, thickness = 1.5 mm, no gap, 256 × 256 matrix, FOV = 240 mm). The Visor 2.0 neuronavigation suite (ANT Neuro, Enschede, the Netherlands) was used for image preprocessing, tissue segmentation, and registration into standard stereotaxic space. The stimulation target was defined in the left DLPFC at MNI coordinate [X-38 Y + 44 Z + 26]

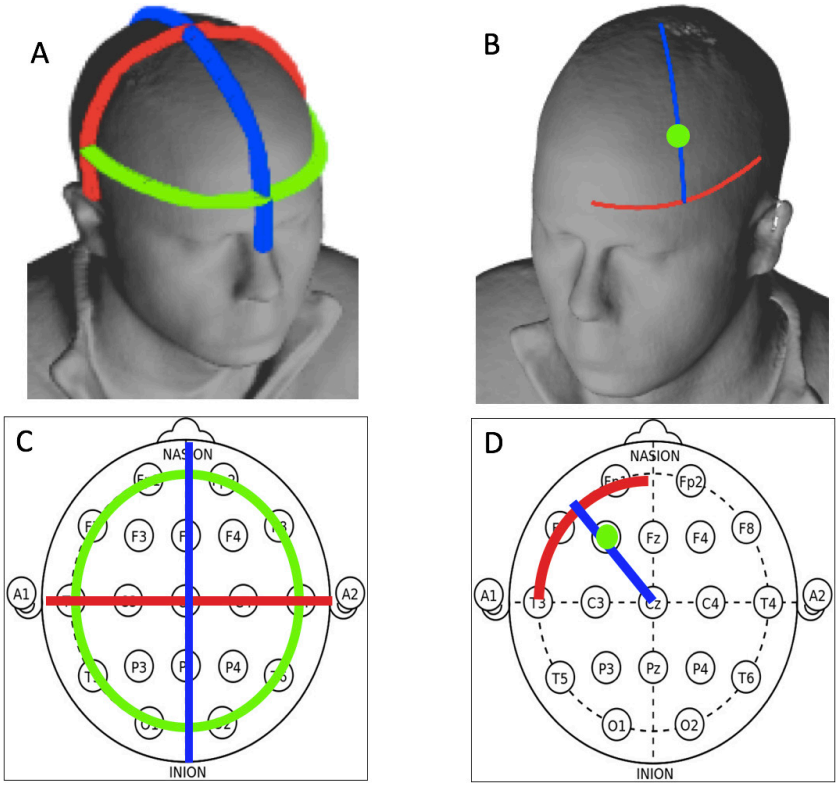

Figure 2. (A) Head circumference; inion-nasion and tragus–tragus distances were measured on the 3D scan of the head using an in-house MATLAB script. (B) These measurements were input into the BeamF3 heuristic [19] (incorporating the +0.35 cm radial extension of Mir-Moghtadaei *et al* [20]) to generate circumferential and radial measures to localize the F3 scalp site, and the script identified the point on the mesh specified by these measures. (C) and (D) Measurement of panels (A) and (B) depicted on a schematic of the international 10–20 EEG montage.

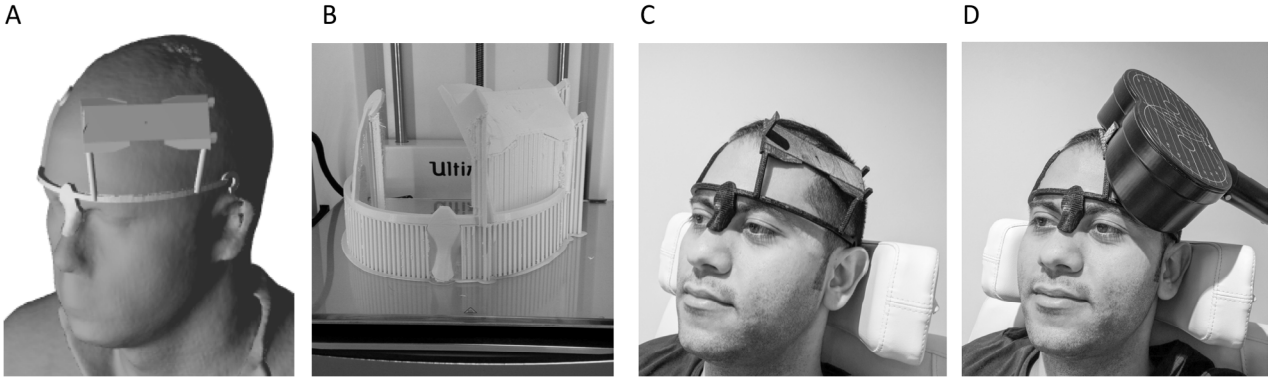

Figure 3. Automated design, fabrication, fitting, and use of the 3D printed rTMS coil-positioning headset. (A) An in-house CAD algorithm generated a headset fitted to the participant's nasion and forehead, incorporating a fitted bracket for holding the coil centred over the F3 location specified in the steps shown in figure 2. (B) The headset was 3D printed in PLA filament on a commercially available 3D printer. (C) The printed headset was positioned on the participant's head to verify a close and comfortable fit and to assess accuracy and reproducibility of specification of the F3 site. (D) During rTMS treatment, the stimulator coil is fitted to the headset to ensure that it is maintained accurately and reproducibly over the desired site of stimulation.

derived from an optimal site identified by Fox *et al* [15], as per our previously published work [20]. The scalp site at minimum Euclidean distance from this point was then localized and marked in the Visor 2.0 software.

Subsequently, the participant donned a fabric neuronavigation cap (MagVenture, Farum, Denmark), and the frameless stereotaxic equipment was used to co-register the participants' head to the MRI using the standard techniques of the Visor 2.0 suite. The sequential steps involved were first placing a headband on the participant's head, attaching a cross with reflective marker spheres to the headband, placing the participant in view of the Visor suite's tracking camera (Polaris Vicra, Northern Digital, Waterloo, Canada), using a pointer also equipped with reflective marker spheres to indicate the positions of the nasion and left and right ear, using the pointer to trace a shell of >50 localization points over the surface of the face and scalp, and finally using the Visor software to co-register these points to the participant's MRI.

Following co-registration, the pointer was used to localize the previously-marked scalp site at minimum distance from the DLPFC target coordinate, as above. Finally, with the pointer maintained in place, the indicated point was marked on the cap on the participant's head using a UV-fluorescent marker. This entire process was timed. The cap and markers were then removed, and the software was completely reset. The method was repeated three times in each participant, to assess the reprodu-cibility of the MRI-guided navigation procedure.

Scalp-landmark method

Each participant donned once again the same fabric cap, and an experienced (>5000 sessions) rTMS technician performed the three cardinal scalp measurements (nasion-inion, tragus–tragus, and head circumference) manually and input these measurements into the BeamF3 algorithm [19] (applying the +0.35 cm radial adjustment of Mir-Moghtadaei *et al* [20]) to generate the circumferential and radial measurements for localizing the DLPFC scalp site. The technician then marked this spot with a different-colored UV-fluorescent invisible marker. This entire process was timed. The cap was then removed, and the entire process was repeated for a total of three times, to assess the reproducibility of the scalp-landmark procedure.

Headset method

Each participant once again donned the same fabric cap, and the technician placed the headset on the patient's head, then marked the spot in the pinhole center of the coil bracket using a different-colored UV-florescent marker. This process was timed. The headset and cap were then removed and all the steps were repeated for a total of three times.

Data analysis

Following completion of all three navigation methods, the invisible markings on the cap were visualized with a UV light source, and marked with a regular visible marker. The caps were then scanned with a commercially available 600 dpi document scanner (Brother MFC-9130WC). A MATLAB script was then applied to the image file, to extract the coordinates of the points marked on the caps and measure their distances relative to each other, and to calculate the centroid of the triangle formed by each set of three points. The centroid of the three MRI navigation measurements was defined as the gold-standard location of the scalp site for all subsequent assessments of accuracy. All statistical comparisons of data during analysis were performed in MATLAB.

Results

Headset fabrication

Headsets took about 12 h to print and were printed overnight to minimize delay to readiness-for-use. About 100 g of standard polylactic acid (PLA) filament was used for printing each headset. PLA filament costs approximately $40 per kilogram and, thus, the cost of material for each headset is about $4. After optimizing the printer and printing settings, there were no failed print attempts.

Table 1. Summary statistics for F3 sites obtained via the MRI-guided, scalp-landmark, and headset methods in terms of accuracy (distance to gold-standard MRI-guided centroid), reproducibility (distance to method's own centroid) and time required to perform each trial of the method. ± values indicate standard deviations from the indicated mean.

	MRI-guided	Scalp landmark	Headset
Distance to MRI-guided centroid			
Mean	3.7 ± 1.6 mm	14.8 ± 7.1 mm	9.7 ± 5.2 mm
Min	1.4 mm	6.0 mm	2.1 mm
Max	7.4 mm	30.4 mm	20.2 mm
Distance from method's own centroid			
Mean	3.7 ± 1.6 mm	4.2 ± 1.4 mm	1.4 ± 0.7 mm
Min	1.4 mm	1.3 mm	0.5 mm
Max	7.4 mm	7.1 mm	3.2 mm
Required time to perform method	113.4 ± 14.9 s	122.9 ± 54.4 s	13.0 ± 5.3 s

Navigation accuracy and reproducibility

For each participant, the gold-standard scalp point was defined as the centroid of the three points obtained by MRI-neuronavigation. Using the MRI-centroid point as the origin, the minimum, mean and maximum distance to the three points obtained via each method was then calculated in each subject as a measure of overall accuracy (table 1).

For MRI-guided neuronavigation, across each of the 20 subjects, the mean distance from MRI-centroid was 3.7 ± 1.6 mm, the minimum distance was 1.4 mm, and the maximum distance was 7.4 mm. For the scalp-landmark BeamF3 method, the mean distance from MRI-centroid was 14.8 ± 7.1 mm, the minimum distance was 6.0 mm, and the maximum distance was 30.4 mm. For the headset method, the mean distance from MRI-centroid was 9.7 ± 5.2 mm, the minimum distance was 2.1 mm, and the maximum distance was 20.2 mm (table 1, figure 4(A)).

As an additional summary statistic, we also calculated 95% confidence ellipses for the overall distribution of points for each method (figures 4(A) and (B)), defining axes along the first and second principal components of the set of all 60 measurements for each modality. Regarding overall accuracy (i.e. in a frame of reference centered with the origin at the MRI-guided centroid for each participant), the axes of the 95% confidence ellipses for each method measured 17.0 mm × 13.8 mm for MRI-guidance, 50.8 mm × 40.9 mm for the BeamF3 method, and 43.2 mm × 27.5 mm for the headset method (figure 4(A)). Regarding reproducibility (i.e. in a frame of reference centered separately for each method, with the origin at the centroid of its own method for each participant), the axes

of the 95% confidence ellipses for each method measured 17.0 mm × 13.8 mm for MRI-guidance, 19.3 mm × 13.3 mm for the BeamF3 method, and 8.0 mm × 2.6 mm for the headset method (figure 4(B)).

Considering all 60 measurements of distance from the MRI-centroid in each modality (within-subject accuracy), there was a significant effect of positioning method ($F(2,52) = 22.95$, $p < 0.0001$). Post-hoc comparison using Tukey's multiple comparison showed accuracy was significantly better for the MRI-guided over the BeamF3 method ($M = -11.0$, $p < 0.0001$), for the headset over the BeamF3 method ($M = 5.1$, $p = 0.008$), and for the MRI-guided over the headset method ($M = -6.0$, $p = 0.0016$).

We next assessed the significance of the differences in reproducibility, calculated as the distance of each measurement from the centroid of its own modality, for each of the 20 subjects. For the BeamF3 method, the mean distance from BeamF3-centroid was 4.2 ± 1.4 mm, the minimum distance was 1.3 mm, and the maximum distance was 7.1 mm. For the headset method, the mean distance from headset-centroid was 1.4 ± 0.7 mm, the minimum distance was 0.5 mm, and the maximum distance was 3.2 mm. (table 1, figure 4(D); *N.B.*, for MRI-neuronavigation, values are as already given above). Reproducibility showed significant differences across navigation methods ($F(2,57) = 27.35$, $p < 0.0001$). Post-hoc comparisons via Tukey's multiple comparison showed that reproducibility was significantly better for the headset over BeamF3 method ($M = 2.8$, $p < 0.0001$) and for the headset over the MRI-guided method ($M = 2.3$, $p < 0.0001$), but not significantly better for the MRI-guided over the BeamF3 method (Tukey's multiple comparison, $M = -0.5$, $p = 0.45$).

Across each of the 20 subjects, the average time required to complete the procedure was 113.4 ± 14.9 s for MRI-guidance, 122.9 ± 54.4 s for the BeamF3 method, and 13.0 ± 5.3 s for the headset method (table 1, figure 4(E)). The time requirements were significantly different between the groups ($F(2,52) = 69.42$, $p < 0.0001$). Post-hoc Tukey's comparisons indicated that the time requirement was significantly shorter for the headset method over either the MRI-guided method ($M = 100.4$, $p < 0.0001$) or the BeamF3 method ($M = 109.9$, $p < 0.0001$), but not significantly different for the MRI-guided versus the BeamF3 method ($M = -9.5$, $p = 0.63$).

Discussion

Although MRI-guided neuronavigation can be considered the gold standard for maximizing the accuracy of rTMS coil placement, logistical obstacles may render this technique impractical in many therapeutic settings, particularly for clinics outside academic or research centers. Scalp-based heuristics such as BeamF3 [19] are available for specific commonly-used targets such as the DLPFC, and may show fairly good concordance with MRI-guided neuronavigation [20] where the latter is unavailable. Yet, scalp-based heuristics are dependent on operator skill, and reproducibility may be variable both across operators and across repeated measurements. Thus, a niche exists for a technique that is less logistically demanding than frameless MRI-guided stereotaxy, yet more reproducible and less reliant on operator skill than manual scalp measurement heuristics.

The 3D-printed headsets described here are offered as a novel neuronavigational technique for achieving high reprodu-cibility and ease-of-use, with low cost and logistical burden. The 3D scanner and printer used here are commercially available at a collective cost <$5000, with the PLA material cost at <$4 per headset, and a single system is capable of fabricating 1 headset per day. MRI is not required, and the head-scanning procedure is rapid and straightforward. Placement of the headset takes on the order of 15 s, versus ~2 min for scalp measurement or MRI-guidance with an experienced operator. Although the fabric caps commonly used for clinical rTMS may also be donned rapidly, they still require the operator to position the coil manually over the marked region and maintain it there throughout treatment, leaving open the possibility of operator error in positioning the coil, or coil drift during treatment due to subject head motion. In contrast, the form-fitted headset's coil bracket ensures that the coil is in the same orientation and position on every session, while minimizing relative motion between the coil and the patient, with less dependence on operator skill and vigilance.

Regarding accuracy (figure 4(A)), the results of the present study showed that the 3D headsets are significantly closer to the MRI-guided gold standard than standard BeamF3 measurements, albeit less accurate than MRI-guidance itself (as might be expected given that MRI-guidance was used to define the site of optimal accuracy). Regarding reproducibility, the 3D headsets actually showed significantly better consistency of positioning than either the scalp-landmark or the MRI-guided methods (figure 4(B)). The latter finding may be explained by the tolerances of calibration for MRI-neuronavigation using the frameless stereotaxy system, which allows up to 3 mm error variance in coil position calibration and up to 3 mm error variance in coil-to-target matching during stimulation. In contrast, the within-subject reproducibility of stimulation site for the form-fitted headset was measured at 1.4 mm ± SD0.7 mm in the present study.

Overall, the headset method permits accuracy intermediate between scalp-landmark and MRI-neuronavigated methods, while achieving reproducibility superior to either method. Of note, a 'hybrid method' could potentially achieve both the high accuracy of MRI-guidance, and the high reproducibility of the headset method, by 3D printing a headset that is centered on an MRI-specified site of stimulation, rather than on the site specified by the BeamF3 heuristic, as in the present study. This straightforward extension is beyond the scope of the present study, but would require only minor modification of the CAD algorithm.

Another straightforward extension of the CAD algorithm would be to substitute alternative coil brackets to hold other rTMS coils. In principle, any coil of any shape by any manufacturer (with the exception of whole-head helmet coils) could be readily accommodated. Going beyond rTMS coils, it is also straightforward to substitute brackets for tES electrodes into the headsets. tES headsets, being closely formed to the patient's head and easy to use, could likely

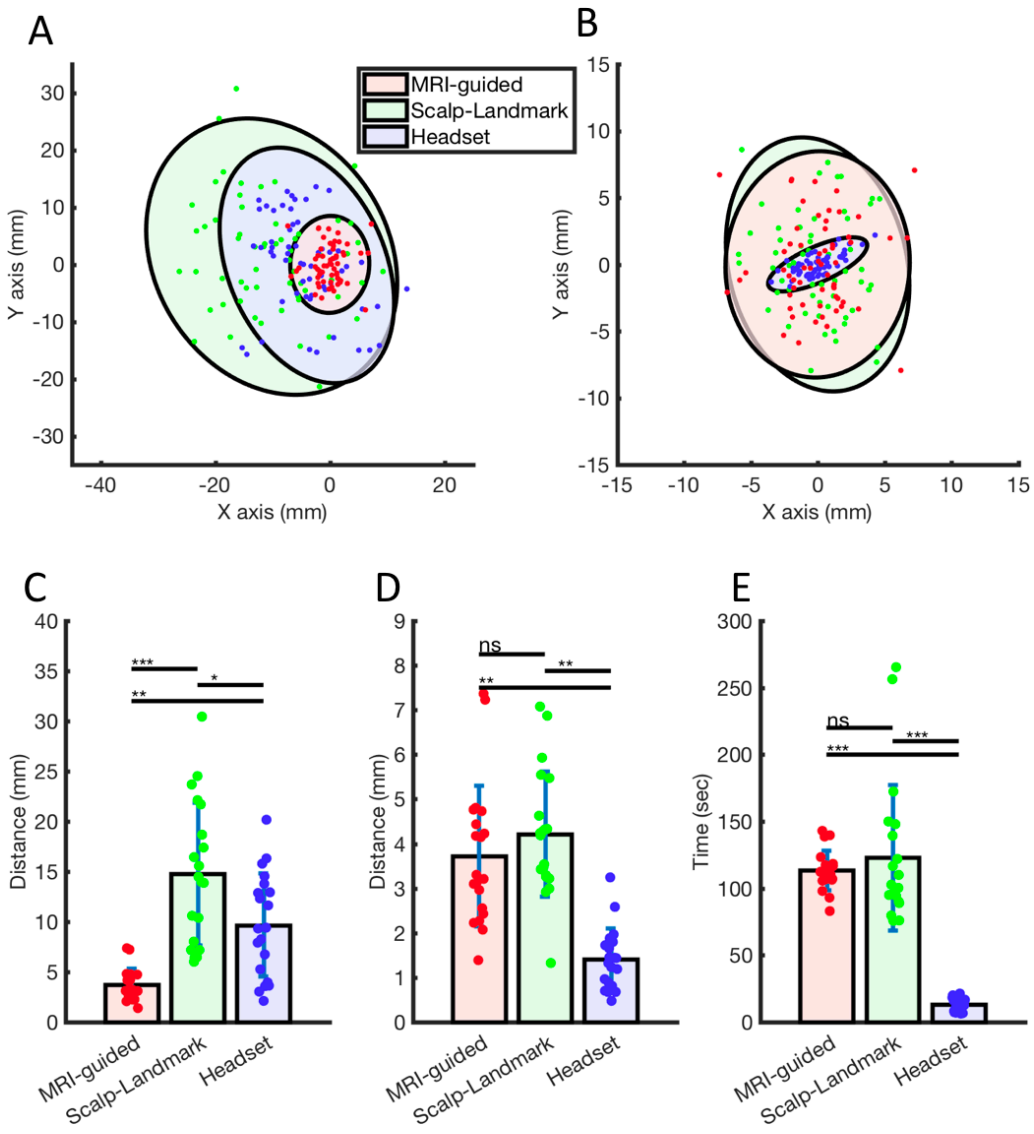

Figure 4. Tukey's multiple comparison was done for all the groups ($*p < 0.01$, $**p < 0.001$, $***p < 0.0001$) (A) Measurements for 3 methods from all the 20 subjects; each method was repeated for each subject three times (60 points for each method). Centroid of MRI-guided method for each subject is used to superimpose the measurements. (B) 95% confidence ellipses for each group. (C) Mean and standard deviation of the distance of each measurement from the center of the MRI-guided method. (D) The distance of each measurement from the center of its own modality. This measures the repeatability of the method in each subject. (E) Average time taken to perform the positioning for each method.

be emplaced correctly by the patients themselves, without the need for an in-clinic operator. This would enable simple, reliable, accurate self-emplacement of tES electrodes by patients without requiring a clinic visit. 3D-printed tES headsets could thus solve one of the potential objections to home-based tES, by ensuring user-friendly, reproducible electrode placement at any desired location on the scalp, once the accurate fit of the headset has been verified in clinic in an initial instructional session. tES brackets printed from an electrical insulator (such as the PLA material of the present study) could also potentially be used to sculpt the electrical field applied to the scalp by the tES electrodes. Similarly, since PLA is non-transparent, specially designed PLA brackets might also be used with optical laser stimulation to sculpt the light field and modulate the dose and depth of stimulation.

Limitations of the present study include the relatively small sample size for the validation, which precludes an empirical re-assessment of the concordance between BeamF3 and MRI-guided methods. As per Mir-Moghtadaei *et al* [20], a larger sample of ~100 would have enabled empirical derivation of a scalp heuristic for left DLPFC; however, such work is beyond the scope of the present study. Another limitation is that the method applies specifically to left DLPFC; other scalp targets would require adjustment of the algorithm and a different design for the headset, depending on location. Another limitation is that the CAD algorithm is designed for a specific coil, although extension to other coils or to tES electrodes is certainly feasible, as above. Finally, a practical limitation is that some expertise is required in MATLAB and in 3D printer maintenance and operation in order to correctly fabricate the headsets. A more user-friendly version with a fully integrated

software workflow, intuitive graphical user interface, and a highly reliable 3D printer may be considered a development project for future work, based on demonstration of the prototype presented in this study. Finally, the impact of coil placement with the 3D headsets on clinical outcomes is unknown. Future studies should consider the randomizing patients to a variety of neuronavigational targeting strategies to determine the optimal method in terms of antidepressant outcome.

In conclusion, the problem of simple, reliable, yet accurate neuronavigation applies both to high-volume therapeutic rTMS clinics and potentially to enabling at-home implementation of therapeutic tES, both of which could greatly improve the accessibility and cost of therapeutic brain stimulation in major depression. The present technique offers a demonstration of the potential utility of low-cost, commercially available 3D scanning, 3D printing, and CAD tools for fabricating neuronavigation aids that exceed MRI-guidance in reproducibility and time-of-implementation, while also exceeding scalp-landmark heuristics in accuracy and reproducibility. Although the presently described headset-creation tool should be considered a prototype, development work would be fairly straightforward to refine the technique for routine, user-friendly use in clinical populations.

Acknowledgment

The authors have confirmed that any identifiable participants in this study have given their consent for publication.

Funding sources

The work was supported by a MITACS Accelerate Grant (#IT05799) to author FM.

ORCID iDs

Farrokh Mansouri https://orcid.org/0000-0002-9814-4971
José Zariffa https://orcid.org/0000-0002-8842-745X
Peter Giacobbe https://orcid.org/0000-0002-2403-5342
Jonathan Downar https://orcid.org/0000-0002-5140-174X

References

[1] McClintock S M *et al* 2018 Consensus recommendations for the clinical application of repetitive transcranial magnetic stimulation (rTMS) in the treatment of depression *J. Clin. Psychiatry* **79** 16cs10905
[2] Milev R V *et al* 2016 Canadian network for mood and anxiety treatments (CANMAT) 2016 clinical guidelines for the management of adults with major depressive disorder: section 4. Neurostimulation treatments *Can. J. Psychiatry* **61** 561–75
[3] Lefaucheur J P *et al* 2014 Evidence-based guidelines on the therapeutic use of repetitive transcranial magnetic stimulation (rTMS) *Clin. Neurophysiol.* **125** 2150–206
[4] Loo C K, Alonzo A, Martin D, Mitchell P B, Galvez V and Sachdev P 2012 Transcranial direct current stimulation for depression: 3-week, randomised, sham-controlled trial *Br. J. Psychiatry* **200** 52–9
[5] Brunoni A R, Valiengo L, Baccaro A, Zanão T A, De Oliveira J F, Goulart A, Boggio P S, Lotufo P A, Benseñor I M and Fregni F 2013 The sertraline versus electrical current therapy for treating depression clinical study *JAMA Psychiatry* **70** 383–91
[6] Brunoni A R *et al* 2017 Trial of electrical direct-current therapy versus escitalopram for depression *New Engl. J. Med.* **376** 2523–33
[7] Shiozawa P, Fregni F, Benseñor I M, Lotufo P A, Berlim M T, Daskalakis J Z, Cordeiro Q and Brunoni A R 2014 Transcranial direct current stimulation for major depression: an updated systematic review and meta-analysis *Int. J. Neuropsychopharmacol.* **17** 1443–52
[8] Brunoni A R *et al* 2016 Transcranial direct current stimulation for acute major depressive episodes: meta-analysis of individual patient data *Br. J. Psychiatry* **208** 522–31
[9] Wang X, Tian F, Reddy D D, Nalawade S S, Barrett D W, Gonzalez-Lima F and Liu H 2017 Up-regulation of cerebral cytochrome-c-oxidase and hemodynamics by transcranial infrared laser stimulation: a broadband near-infrared spectroscopy study *J. Cereb. Blood Flow Metab.* **37** 3789–802
[10] Wang X, Dmochowski J, Husain M, Gonzalez-Lima F and Liu H 2017 Proceedings #18. Transcranial infrared brain stimulation modulates EEG alpha power *Brain Stimul.* **10** e67–9
[11] Tufail Y, Yoshihiro A, Pati S, Li M M and Tyler W J 2011 Ultrasonic neuromodulation by brain stimulation with transcranial ultrasound *Nat. Protocols* **6** 1453–70
[12] Berlim M T, van den Eynde F, Tovar-Perdomo S and Daskalakis Z J 2014 Response, remission and drop-out rates following high-frequency repetitive transcranial magnetic stimulation (rTMS) for treating major depression: a systematic review and meta-analysis of randomized, double-blind and sham-controlled trials *Psychol. Med.* **44** 225–39
[13] Berlim M T, Van den Eynde F and Daskalakis Z J 2013 Clinically meaningful efficacy and acceptability of low-frequency repetitive transcranial magnetic stimulation (rTMS) for treating primary major depression: a meta-analysis of randomized, double-blind and sham-controlled trials *Neuropsychopharmacology* **38** 543–51
[14] Berlim M T, Van Den Eynde F and Daskalakis Z J 2013 A systematic review and meta-analysis on the efficacy and acceptability of bilateral repetitive transcranial magnetic stimulation (rTMS) for treating major depression *Psychol. Med.* **43** 2245–54
[15] Fox M D, Buckner R L, White M P, Greicius M D and Pascual-Leone A 2012 Efficacy of transcranial magnetic stimulation targets for depression is related to intrinsic functional connectivity with the subgenual cingulate *Biol. Psychiatry* **72** 595–603
[16] Downar J, Blumberger D M and Daskalakis Z J 2016 The neural crossroads of psychiatric illness: an emerging target for brain stimulation *Trends Cogn. Sci.* **20** 107–20
[17] Herbsman T, Avery D, Ramsey D, Holtzheimer P, Wadjik C, Hardaway F, Haynor D, George M S and Nahas Z 2009 More lateral and anterior prefrontal coil location is associated with better repetitive transcranial magnetic stimulation antidepressant response *Biol. Psychiatry* **66** 509–15
[18] George M S, Wassermann E M, Williams W A, Callahan A, Ketter T A, Basser P, Hallett M and Post R M 1995 Daily repetitive transcranial magnetic stimulation (rTMS) improves mood in depression *Neuroreport* **6** 1853–6
[19] Beam W, Borckardt J J, Reeves S T and George M S 2009 An efficient and accurate new method for locating the F3

position for prefrontal TMS applications *Brain Stimul.* **2** 50–4

[20] Mir-Moghtadaei A, Caballero R, Fried P, Fox M D, Lee K, Giacobbe P, Daskalakis Z J, Blumberger D M and Downar J 2015 Concordance between BeamF3 and MRI-neuronavigated target sites for repetitive transcranial magnetic stimulation of the left dorsolateral prefrontal cortex *Brain Stimul.* **8** 965–73

[21] Nemeroff C B 2007 Prevalence and management of treatment-resistant depression *J. Clin. Psychiatry* **68** 17–25 (www.psychiatrist.com/jcp/article/Pages/2007/v68s08/v68s0803.aspx)

[22] Cignoni P *et al* 2008 MeshLab: an open-source mesh processing tool *Sixth Eurographics Italian Chapter Conf.* pp 129–36